5-2014

Cd dipping to reduce reactivity of fuel assemblies in spent fuel pools

John Clark Stooksbury
jstooks9@utk.edu

Nuclear System Design: Cd Dipping to Reduce Reactivity of Fuel Assemblies in Spent Fuel Pools

Trevor L. Binkley
Preston W. Carroll
Raymond E. Flanery
John C. Stooksbury
Zach Welz
Thomas S. Wood VI

Friday, April 25, 2014

Contents

List of Figures

Appendices

1: Abstract

Used Nuclear Fuel (UNF) requires special treatment throughout its lifetime. From the fuel pool to geologic disposition, the hazards of UNF are continually managed. The challenges encountered in the establishment of a permanent High Level Waste (HLW) repository in the US have led to increased demand for temporary onsite storage of UNF at reactor sites. The limited area available to store UNF dictates efficient storage be rewarded. Criticality safety and cooling of UNF limit the degree to which assemblies may be packed however. Fuel pools make use of neutron absorbers plates in their storage racks to decrease required space among assemblies. An alternative method is proposed to aid in the packing of UNF assemblies. After adequate cooling time, an assembly could be temporarily removed from the used fuel pool and dipped in a neutron absorbing metal and then replaced in the pool. The assembly retains the added negative reactivity after pool removal and placement into dry cask storage. Among multiple neutron absorbers investigated, only pure Cadmium wetted on zircaloy used in common nuclear fuel designs. A numerical 1-D thermal analysis of a fuel element found that the rate at which an assembly heats in air restricts the earliest elapsed time required after reactor removal to perform the dipping process. Criticality analysis using SCALE 6.1 found that with the cadmium shell, as time increases, K_{eff} tends to decrease overall. An exponential decrease of K_{eff} as the thickness of the cadmium shell is increased was found. The K_{eff} of the spent fuel pool approaches an asymptote at approximately 0.2 at a cadmium shell thickness of approximately 0.025 cm. The K_{eff} of the dry storage cask approaches an asymptote at approximately 0.2 at a cadmium shell thickness of approximately 0.05 cm. The evaluations of a neutron absorbing shell show that the application of such a shell is feasible and useful when applied to UNF assemblies.

2: Introduction

Reactor operators manage Used Nuclear Fuel (UNF) from the moment it leaves the reactor core. Currently UNF assemblies reside in a water-filled pool until the decay heat output of the individual assembly decreases to more manageable levels. The Nuclear Regulatory Commission (NRC) authorizes spent fuel to be removed from the pool after a minimum of three years, but the industry norm is around ten years. Then the assembly is bundled with other assemblies in a dry storage cask indefinitely. In the US, casks reside at an Independent Spent Fuel Storage Installation (ISFSI). As of March 2013, 54 general licensed ISFSIs are operating; 9 reactor sites are pursuing a general licensed ISFSI; and 15 specific licensed ISFSIs are opened. FIGURE 1 shows the location of ISFSIs in the US. The need for more ISFSIs increases as UNF pools fill to capacity. FIGURE 2 shows this trend and the projected number of pools filling in coming years.[1] These factors raise the value of space in UNF pools greatly. Therefore there is a desire to keep assemblies as close together as safely possible.

Figure 1: ISFSI sites in the US.[1]

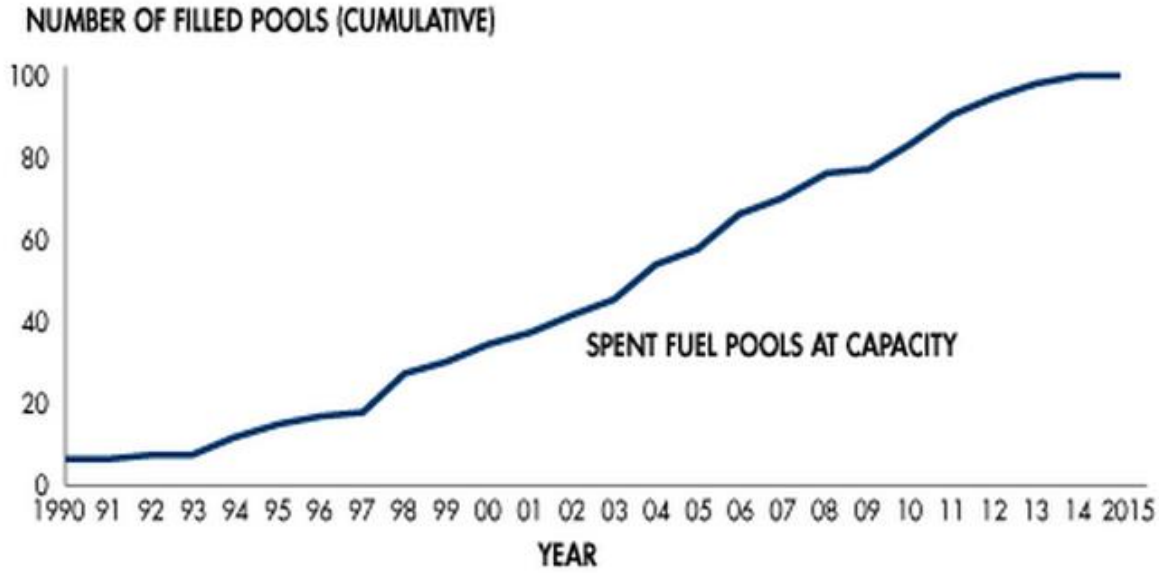

Figure 2: Spent fuel pools at capacity from 1990-2015 (later data projected).[1]

Currently, neutron absorbing plates, made of materials such as BORAL, are used as negative reactivity worth in UNF management to control criticality of assemblies[2]. This plating allows for less spacing between assemblies than the case without BORAL. While this is an effective strategy to reduce reactivity in the pool and beyond, such plates could be eliminated by the addition of a neutron absorbing shell surrounding each fuel pin in an assembly. This work proposes that UNF be temporarily removed at a point when the fuel produces sufficiently low heat that the assembly can be dipped in a neutron absorbing metal which then wets to the zircaloy surfaces of fuel pins to form a shell. Then the

assembly is lowered back into the pool for more compact and safer storage. The integrity of the proposed absorber is evaluated both in the cooling pool and in dry cask storage. A criticality analysis is then performed to determine the benefit of utilizing the proposed dipping/wetting process. Multiple alloys and metals are explored to determine a suitable shell candidate material. A small sample of zircaloy is dipped into a melted mass of the tested shell material and then checked for wetting. Once a suitable material is found, all evaluations are performed to determine the plausibility of the material for sustained presence on the fuel pins.

Using a small furnace and samples of Cd, Pb, and Zn, zircaloy samples were dipped in Cd, Cd-Pb, and Cd-Zn alloys. The only metal found to wet was pure Cd, shown in Figure 3 below.

Figure 3: Cd wetted on a zircaloy rod. The rod was dipped while the Cd was near its melting point, 321.1 °C.

Wetting is important to this design because it is required in order to make a braze/solder joint. This joining occurs when the filler metal (cadmium) wets the base metal (zircaloy) by way of a surface energy gradient.[7] Other alloys attempted were Pb-17Cd and Cd-17Zn. Being the only successful absorber/filler metal to wet, all evaluations are performed using a Cd neutron-absorbing shell. Measurements of the Cd deposit thickness were sampled along the radius of the cylinder, and the Cd was found to deposit, on average, with a thickness of 1 mm. The shell is non-uniform, but is approximately 1 mm in thickness at all points.

3: Thermal Analysis

The following thermal analysis is conducted as a conservative estimate for thermal conditions both within a spent fuel pool and dry cask storage. Each equation uses the max allowable non-accident scenario coolant temperature each shown in Table 1.

Table 1: Maximum allowable temperature for storage coolants

Location	Coolant	Max Temp (C)
Spent Fuel Pool	Water	50
Dry Cask Storage	He	197.4

The following equations are developed for a one-dimensional assessment of a single fuel pin. Adjacent heating due to neighboring fuel pins is assumed to be negligible and is therefore not considered. Specific assumptions for individual regions of analysis are discussed as they become relevant throughout the analysis below.

The purpose of this thermal analysis is to develop a set of equations governing the heat transfer throughout the fuel pin. This allows for the determination of an optimum time to apply an alloy shell to a UNF assembly while retaining the integrity of the shell and preventing the existing zircaloy cladding from melting. The established equations are then implemented into a FORTRAN 95 program, which solves for steady-state and transient temperature profiles within the UNF pin.

The general equation governing heat transfer within each of the fuel pin regions is:

$$\frac{1}{r}\left(\frac{d}{dr}\right)K_x r\left(\frac{dT}{dr}\right) = -q'' \quad (1)$$

Where:

r = radius [cm]
K = thermal conductivity of the material [$W*cm^{-1}*K^{-1}$]
x = specified region of interest (f = fuel, g = gap, c = clad, s = shell).
T = temperature [Celsius]
q'' = area heat generation [$W*cm^{-2}$]

Assumptions include continuity between the boundaries (i.e. at fuel-gap boundary $q''_{fuel} = q''_{gap}$) as well as no heat generation outside of the fuel region. Therefore, the resulting equations for the interior nodes are discussed below.

To determine governing equations within the fuel, equation 1 is integrated across the fuel region.

$$\int_{r_i-\frac{\Delta r_f}{2}}^{r_i+\frac{\Delta r_f}{2}} \frac{d}{dr} K_f r \frac{dT}{dr} = \int_{r_i-\frac{\Delta r_f}{2}}^{r_i+\frac{\Delta r_f}{2}} -q'''rdr \quad (2)$$

Where:

r_i = radius of the i^{th} node [cm]
q''' = volumetric heat generation [$W*cm^{-3}$]

Equation 2 is integrated and then reduced to a form which is divided into temperature groups.

$$[\frac{K_f}{r_i \Delta r_f^2}(r_i - \frac{\Delta r_f}{2})]T_{i-1} - [\frac{2K_f}{\Delta r_f^2}]T_i + [\frac{K_f}{r_i \Delta r_f^2}(r_i + \frac{\Delta r_f}{2})]T_{i+1} = q''' \quad (3)$$

Where:

T_{i-1} = temperature of the previous node
T_i = temperature of the current node
T_{i+1} = temperature of the next node

The coefficients for each temperature group can then be calculated and the heat rate in the fuel region can be determined through iterative methods.

The first section for thermal analysis is the fuel centerline. The major assumption of the fuel centerline node is that it has the maximum temperature throughout the fuel pin ($\frac{dT}{dr} = 0$ at $r = 0$). Equation 1 is then integrated over the centerline boundaries.

$$\int_0^{\frac{\Delta r_f}{2}} \frac{d}{dr} K_f r \frac{dT}{dr} = \int_0^{\frac{\Delta r_f}{2}} -q'''rdr \quad (4)$$

The results of integrating equation 4 are then reduced into temperature groups.

$$[\frac{4K_f}{\Delta r_f^2}]T_i - [\frac{4K_f}{\Delta r_f^2}]T_{i+1} = q''' \quad (5)$$

Nodes within the gap, clad, and shell are all assumed to have zero heat generation, and are therefore treated similarly, varying only in conduction coefficient (K_x) and nodal spacing (Δr_x). For each section, equation 1 is integrated over the region boundaries.

$$\int_{r_i-\frac{\Delta r_x}{2}}^{r_i+\frac{\Delta r_x}{2}} \frac{d}{dr} K_x r \frac{dT}{dr} = 0 \quad (6)$$

where subscript x is a placeholder for the region of interest (f = fuel, g = gap, c = clad, s = shell) for all variables.

The results of the integration are then reduced into respective temperature groups.

$$\left[\frac{\left(r_i-\frac{\Delta r_x}{2}\right)}{\Delta r_x}\right]T_{i-1}-\left[\frac{2r_i}{\Delta r_x}\right]T_i+\left[\frac{\left(r_i+\frac{\Delta r_x}{2}\right)}{\Delta r_x}\right]T_{i+1}=0 \quad (7)$$

To determine the interface equations, equation 1 is integrated from the last fuel node to the first gap node.

$$\int_{r_i-\frac{\Delta r_x}{2}}^{r_i+\frac{\Delta r_x}{2}} \frac{d}{dr}K_x r\frac{dT}{dr}=\int_{r_i-\frac{\Delta r_f}{2}}^{r_i+\frac{\Delta r_f}{2}} -q'''rdr \quad (8)$$

Equation 8 is then integrated, reduced into respective temperature groups, and specific conduction coefficients and nodal spacing values inserted with the assumption of conservation of heat flux.

$$\left[\frac{K_f\left(r_i-\frac{\Delta r_f}{2}\right)}{\Delta r_f}\right]T_{i-1}-\left[\frac{K_f\left(r_i-\frac{\Delta r_f}{2}\right)}{\Delta r_f}+\frac{K_g\left(r_i+\frac{\Delta r_g}{2}\right)}{\Delta r_g}\right]T_i+\left[\frac{K_g\left(r_i+\frac{\Delta r_g}{2}\right)}{\Delta r_g}\right]T_{i+1}$$
$$=-\frac{q'''}{2}\left(r_i\Delta r_f-\frac{\Delta r_f^2}{4}\right) \quad (9)$$

The interface region between the Gap and Clad is similar to the region between the Fuel and Gap, aside from the lack of heat generation and specific conduction coefficients and nodal spacing values.

$$\left[\frac{K_g\left(r_i-\frac{\Delta r_g}{2}\right)}{\Delta r_g}\right]T_{i-1}-\left[\frac{K_g\left(r_i-\frac{\Delta r_g}{2}\right)}{\Delta r_g}+\frac{K_c\left(r_i+\frac{\Delta r_c}{2}\right)}{\Delta r_c}\right]T_i+\left[\frac{K_c\left(r_i+\frac{\Delta r_c}{2}\right)}{\Delta r_c}\right]T_{i+1}=0 \quad (10)$$

The same form applies to the Clad and Shell interface.

$$\left[\frac{K_c\left(r_i-\frac{\Delta r_c}{2}\right)}{\Delta r_c}\right]T_{i-1}-\left[\frac{K_c\left(r_i-\frac{\Delta r_c}{2}\right)}{\Delta r_c}+\frac{K_s\left(r_i+\frac{\Delta r_s}{2}\right)}{\Delta r_s}\right]T_i+\left[\frac{K_s\left(r_i+\frac{\Delta r_s}{2}\right)}{\Delta r_s}\right]T_{i+1}=0 \quad (11)$$

Similar to previous boundaries, the outermost node, which is the Shell-Coolant interface region, begins by integrating equation 1.

$$\int_{r_i-\frac{\Delta r_s}{2}}^{r_i} \frac{d}{dr} K_s r \frac{dT}{dr} = \int_{r_i-\frac{\Delta r_s}{2}}^{r_i} -q'''rdr \quad (12)$$

The furthest reduction step after integration is given as:

$$[K_s r \frac{dT}{dr}]_{r_s}(r_s) - K_s(r_i - \frac{\Delta r_s}{2})(\frac{T_i - T_{i-1}}{\Delta r_s}) = 0 \quad (13)$$

The convective boundary condition $r = r_c$ is then applied where:

$$q_\infty = h_\infty(T_s - T_\infty) = [-K_s \frac{dT}{dr}]_{r_s} \quad (14)$$

Where:

q_∞= rate of heat transfer to the film
h_∞= heat transfer coefficient of the film
T_∞= film temperature

The result is the convective and conductive heat transfer interface equation for the Shell and Coolant.

$$[\frac{K_s}{\Delta r_s}(r_i - \frac{\Delta r_s}{2})]T_{i-1} - [r_i h_\infty + (r_i - \frac{\Delta r_s}{2})]T_i = -r_i h_\infty(T_\infty) \quad (15)$$

To solve these equations at various volumetric heat generation rates, coolant materials, coolant temperatures, shell thicknesses, and other variables, a FORTRAN 95 program was written, which solves for the temperature profile of the fuel pin. The program takes variable inputs from pre-written input decks, and creates output files with the resulting thermal profiles for steady-state (within spent fuel pool) and transient (in air) thermal analysis. The resulting profiles developed using the thermal code are discussed in section 5: Thermal computations and results.

4: Thermal computations and results

Three scenarios are considered for the thermal analysis. Each is evaluated at the maximum allowed coolant temperature, as discussed previously in Table 1. Since only Cd is the sole shell material found to wet with zircaloy, Cd alone is evaluated. The 1-D heat transfer calculation is informed by linear power outputs computed using a point-depletion model in ORIGEN from the SCALE software package.

By evaluating the temperature profile throughout a fuel element at the maximum coolant temperature, the integrity of the Cd shell is assured under normal operating conditions providing that an accident condition is not in effect. Figure 4 shows the radial temperature profile of a fuel element coated in Cd. The data are shown in three-month

increments from initial cooling to five years of residence in the spent fuel pool. The transition from fuel region to gap region is marked by a sudden drop in temperature as the reduced thermal conductivity throttles the heat transfer in the fuel pin. The profile then levels off as the clad and shell regions are entered. While fuel centerline temperature varies greatly as a function of cooling time, clad and shell temperature generally hover near to each other. Figure 5 shows the three-month profile alone and in greater detail. Each material region is clearly seen.

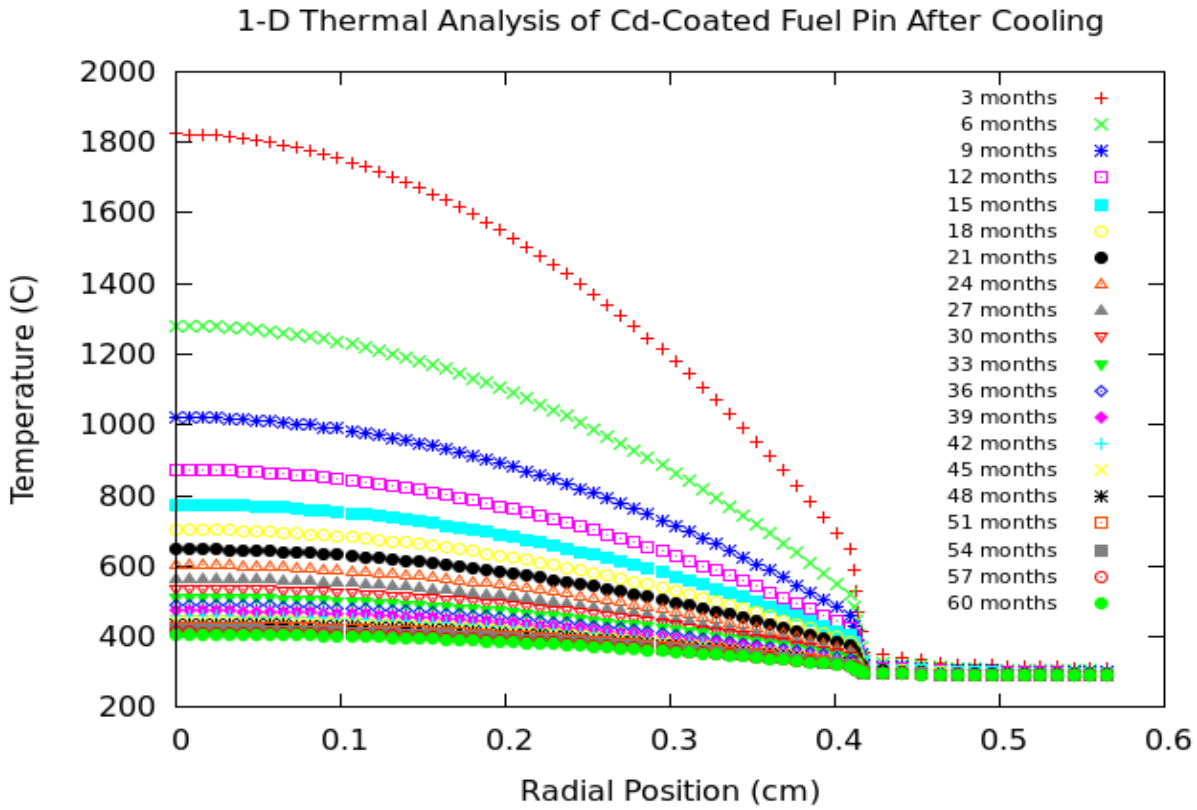

Figure 4: Thermal analysis profile by radial position in the fuel rod.

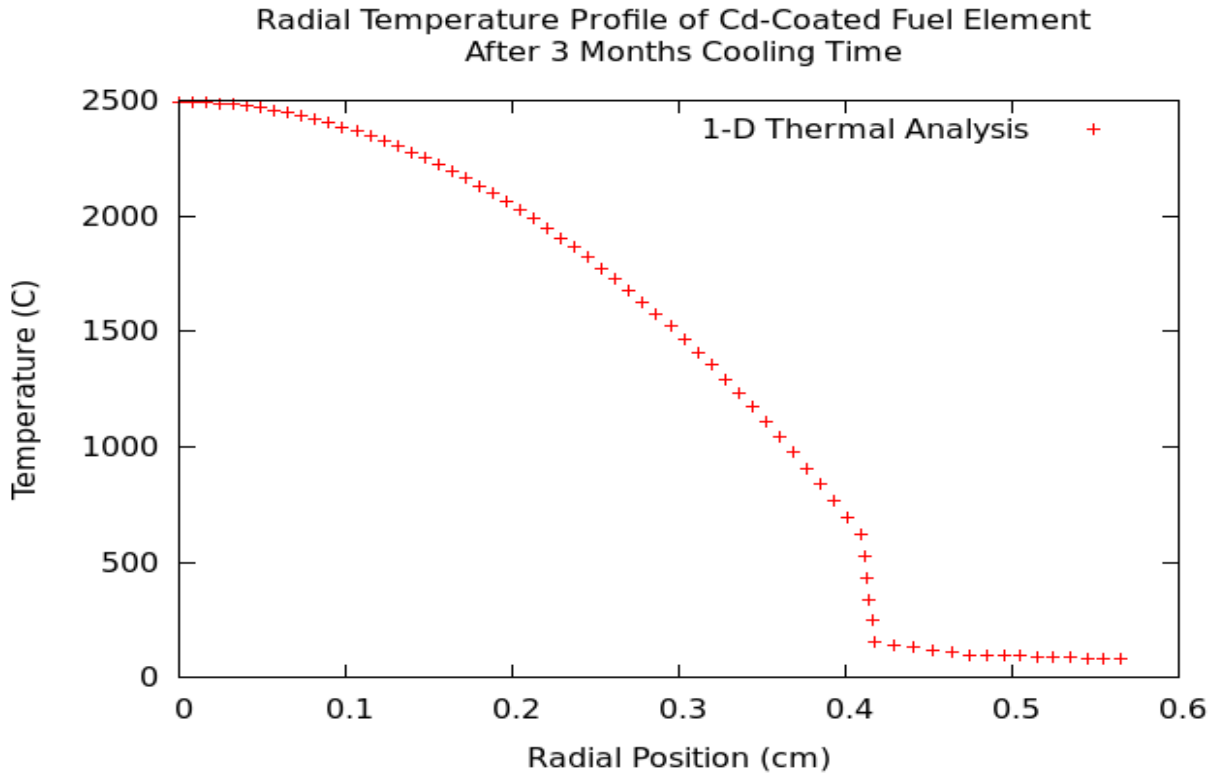

Figure 5: Detailed Graph of Cd coated fuel rod after three months.

Data such as that represented in Figure 5 is calculated for each coolant listed in Table 1 and at the same time intervals as shown in Figure 4. Of most concern is the maximum temperature that the shell material encounters. The maximum safe temperature generally lies 50 C below the melting point of that material. 327.4 C relates to a maximum temperature of 277.4 C for the Cd shell. Figures 6 and 7 show the maximum shell region temperature as a function of cooling time. Only the He coolant approaches the melting point of Cd. This necessitates at least six months cooling prior to placing a dipped assembly into dry cask storage without fear of Cd melting and phase transformations while present of fuel pins in the dry cask. Since an assembly cannot be removed until 3 years has passed regardless, the Cd shell will retain its integrity in a dry storage cask at any point the assembly is even considered for removal from UNF pool. The data for water shows that the assembly is thermally suitable for Cd dipping after 3 months cooling.

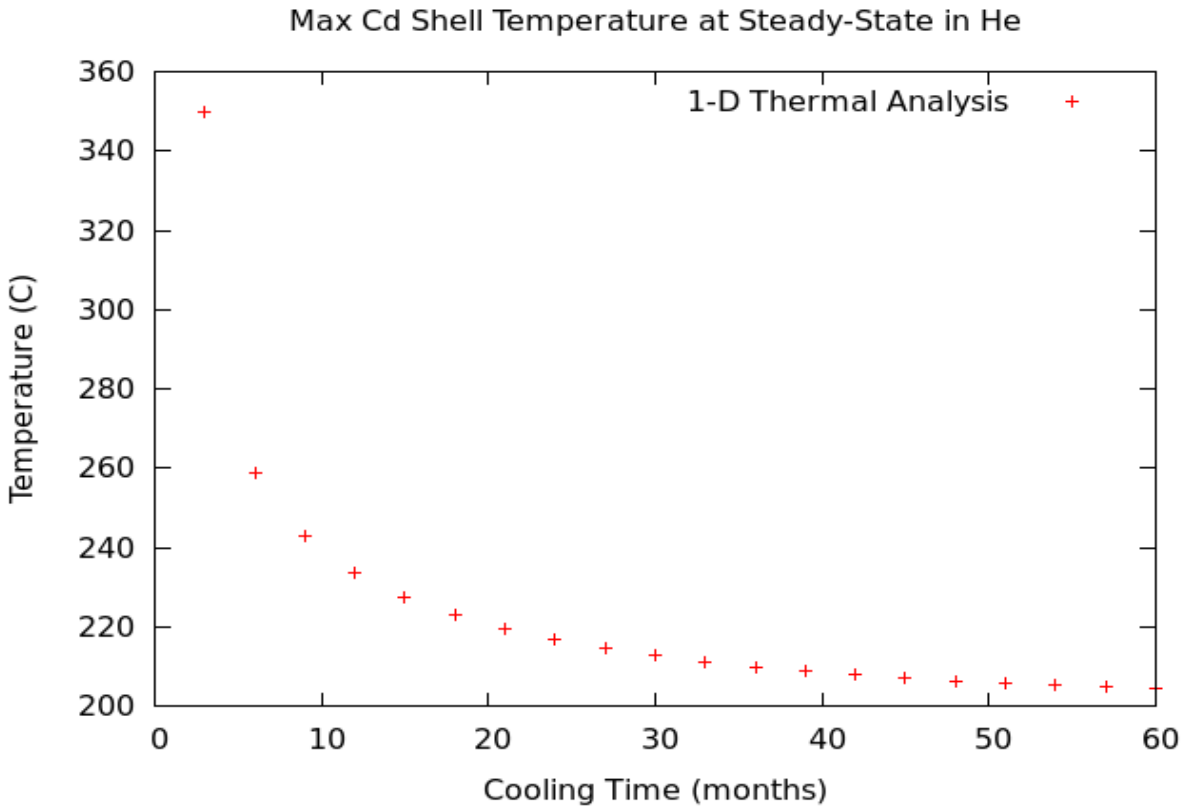

Figure 6: Temperature of fuel rod Cd Shell at steady state in helium versus time after removal from the reactor.

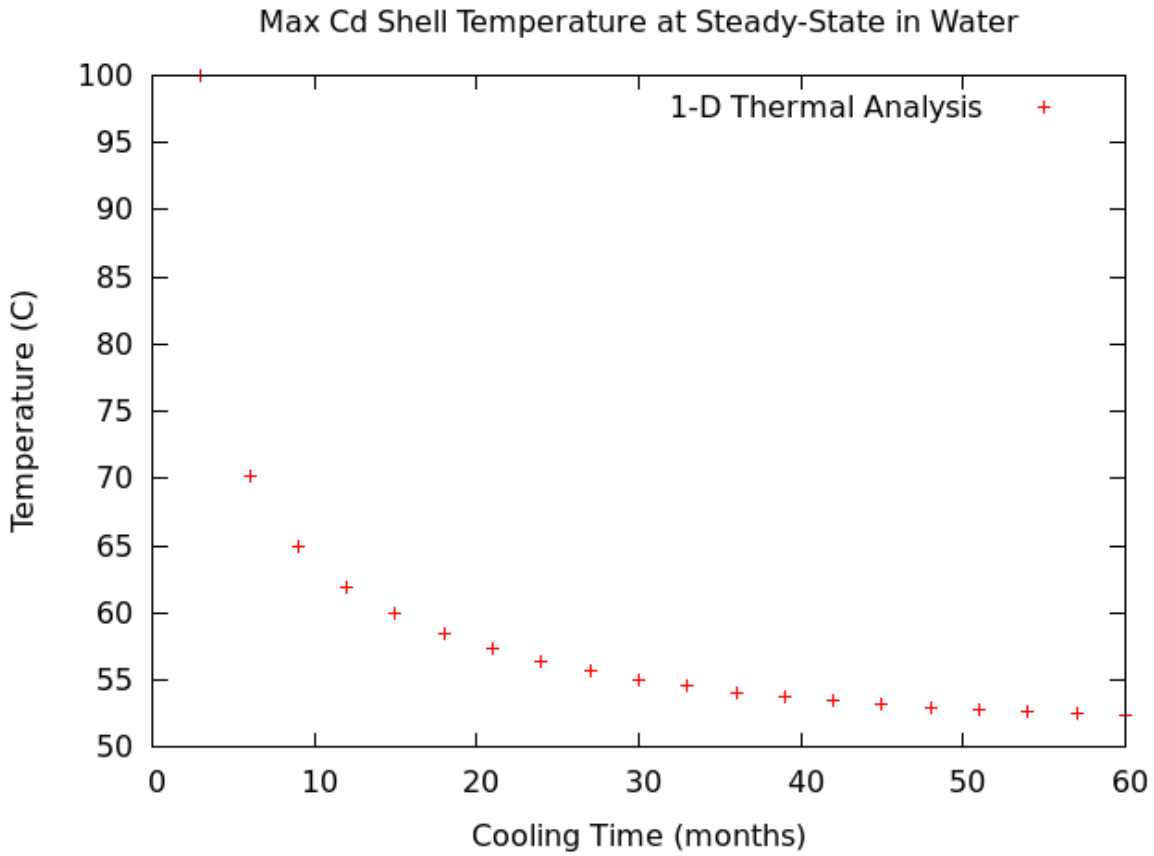

Figure 7: Temperature of fuel rod Cd Shell at steady state in water versus time after removal from the reactor.

In addition to thermal and criticality analyses, an Origen calculation is used to predict the assembly's activity as a function of cooling time. If an apparatus were successfully designed to implement assembly dipping, great challenges are met with shielding the sheer magnitude of activity generated.

5: Criticality

Whenever one is dealing with fissile materials, it is best to do a criticality analysis. This type of analysis ensures that during a given situation, with set parameters, a criticality will not occur. For this project however, we were not concerned with a criticality occurring, but rather with the difference adding a thin shell of cadmium would make to K_{eff}. SCALE 6.1 was used to model the fuel inside a spent fuel pool and inside a storage cask. *"SCALE is a comprehensive modeling and simulation suite for nuclear safety analysis and design developed and maintained by Oak Ridge National Laboratory under contract with the U.S. Nuclear Regulatory Commission, U.S. Department of Energy, and the National Nuclear Security Administration to perform reactor physics, criticality safety, radiation shielding, and spent fuel characterization for nuclear facilities and transportation/storage package designs."*[3]

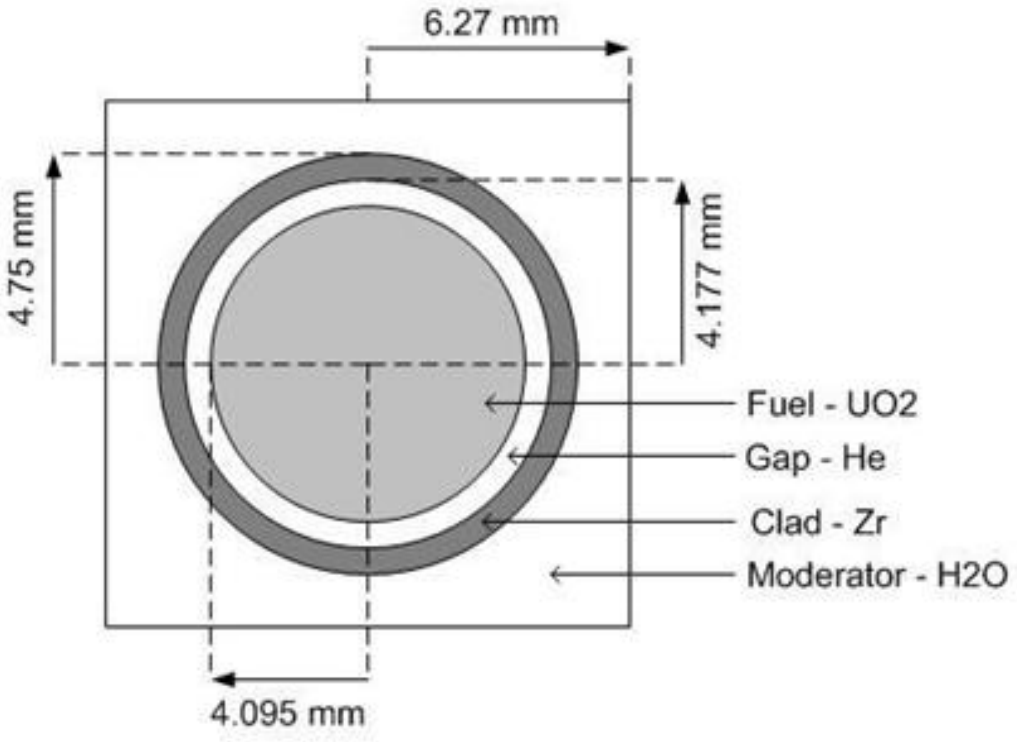

Figure 8: Typical Westinghouse fuel element. [4]

The fuel assemblies are modeled after generic Westinghouse PWR fuel elements in a 17x17 array, as shown in Figure 8. They have a total height of 4 meters. The fuel itself is uranium dioxide (UO2), which is surrounded by a gap of Helium, then a layer of Zircaloy-4. Instrumentation and Control Rod Guide Thimbles were not modeled; this exclusion adds an amount of conservatism to our measurements. For our simulation we used Origin-ARP to get the compositions of fuel that has undergone burnup in three month intervals over the first five years out of the reactor. In order to use these compositions in Scale, we had to create our own material card instead of using a premade one. All assemblies are modeled identically with no variation in burnup.

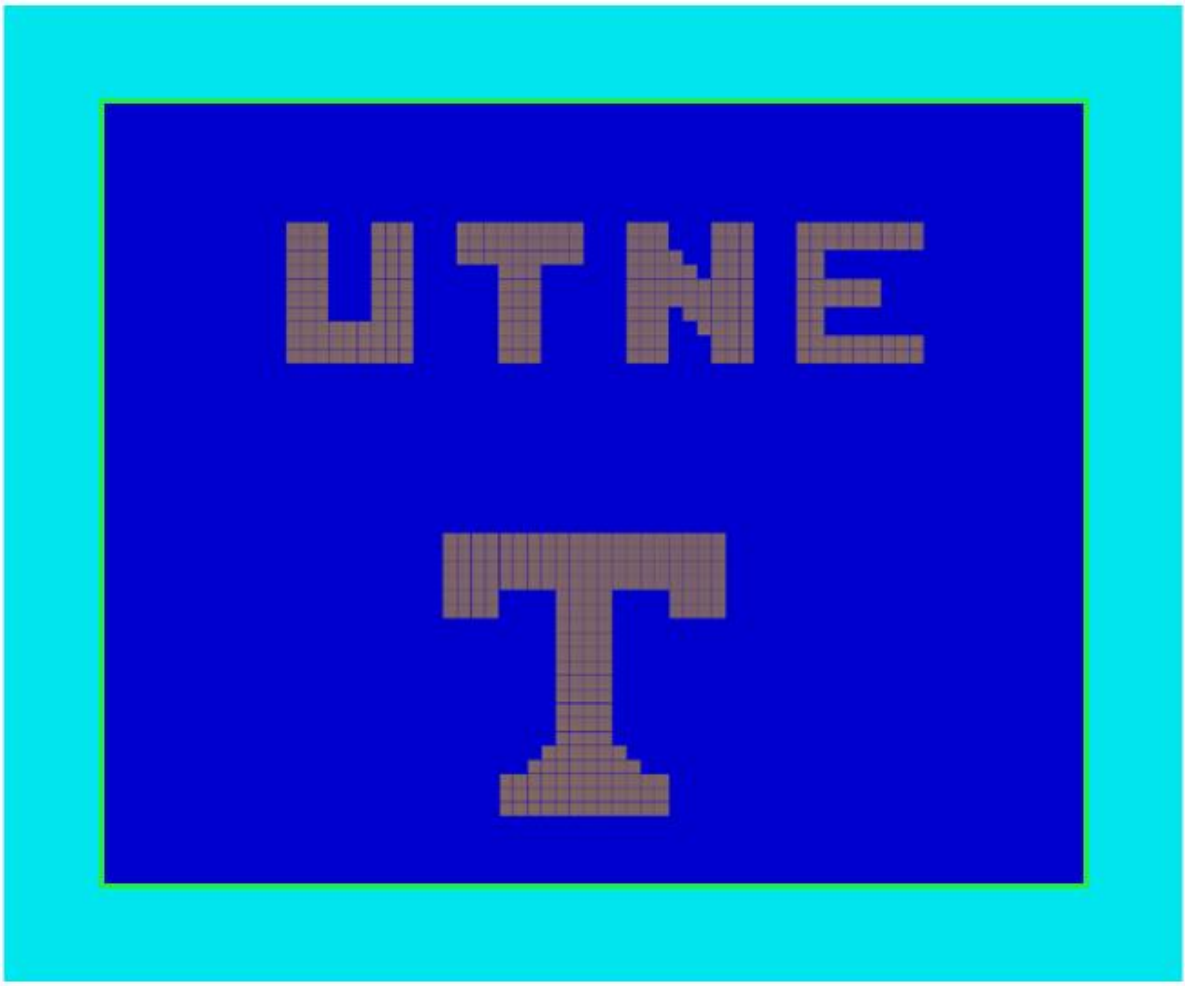

Figure 9: Spent Fuel Pool Model

The spent fuel pool shown in Figure 9 was modeled after generic spent fuel pool dimensions found in NUREG-1738. The light blue is concrete, which is 1.5 meters thick on the sides and 1.2 meters thick on the bottom. This was modeled as reg-concrete, which is Regulatory Concrete that was developed for the U.S. NRC[5]. Moving inwards is the light green, which was added to this figure because it is really so small in comparison to everything else that it cannot be seen, is a 0.00635 meter (1/4") thick stainless steel liner, modeled as SS-304. The dark blue is the water inside the pool with dimensions approximately 15 x 12 x 18 meters. The water does not contain boron as this provides a more conservative simulation. The UTNE and accompanying Power T are the fuel assemblies which are covered with approximately 13 meters of water. This layout was chosen because it is a little more interesting to look at then either filling the pool completely or bunching fuel assemblies into the corner. As stated before, our interests lie purely in the difference between K_{eff} with and without cadmium, not with finding a subcritical layout for the spent fuel pool.

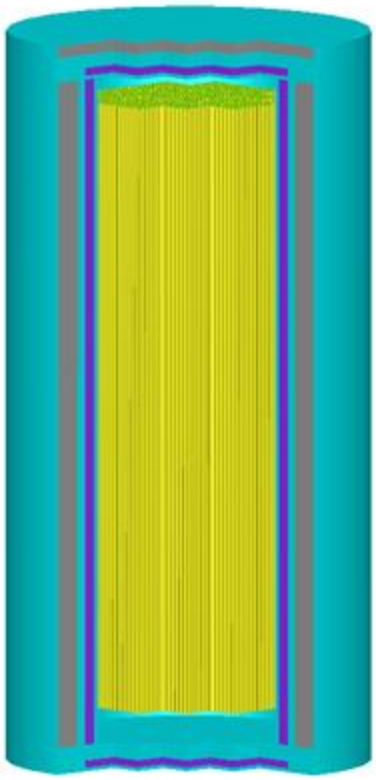

Figure 10: 3D Dry Storage Cask Model

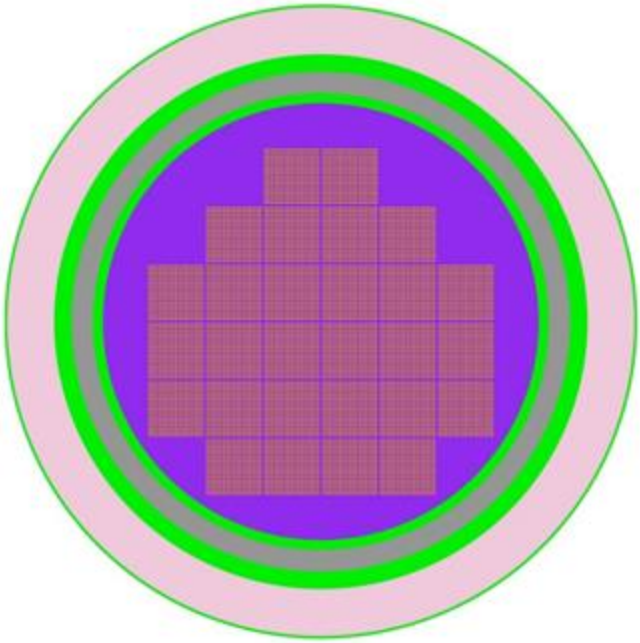

Figure 11: Top-down view of Dry Storage Cask

The dry storage cask shown in Figures 10 and 11 were modeled after the NAC-I28 Dry Storage Cask found in TR-101091. This cask was designed, licensed, and fabricated by the Nuclear Assurance Corporation for use at the Virginia Power Surry Power Station Independent Spent-Fuel Storage Installation. Its first use was in March 1991. The NAC-I28 is designed to hold 28 spent PWR fuel assemblies. The NAC-I28 is approximately 4.4 meters tall and 2.4 meters in diameter.[6]

Figure 10 shows a 3D view of the NAC-I28 Dry Storage Cask, made using KENO3D, in which one can see the 16.5 cm thick stainless steel lid with the purple being a 5.1 cm thick lead gamma shield and the grey is a 7.6 cm 5 wt% borated polyethylene neutron shield. One can also see the 17.7 cm thick bottom with a lead gamma shield which is 4.6 cm thick. [6]

Figure 11 shows a top-down view of the NAC-I28 Dry Storage Cask. In this view one can see (from inside to outside) the fuel assemblies, surrounded by the helium atmosphere, a 3.8 cm thick inner shell of stainless steel, a 8.1 cm thick lead gamma shield, a 6.6 cm thick stainless steel outer shell, a 17.8 cm thick layer of 5 wt% borated polyethylene, finally encased in a 1 cm thick shell of stainless steel. [6]

Simulations were performed using SCALE 6.1 to determine the K_{eff} for the fuel assemblies in both the spent fuel pool and dry storage cask. The CSAS25 sequence was used to allow the use of 3D geometries, using the KENO 3D transport model. NITAWL was used to for resonance processing of resolved resonances. The 44 energy group ENDF5

cross section library was used. The simulations were run for fuel composition at 3, 6, 18, 36, and 60 month intervals with and without a 1 mm cadmium shell. They were also run for varying thicknesses of cadmium from no cladding shell to 1 mm using the 18 months fuel. Fission maps were created for the cases of in the spent fuel pool and in the cask, with and without the cadmium cladding shell. These were created with a few extra lines of code specifying the area over which to create the map. An output file was automatically generated which served as an input file to MeshView, a program that comes as part of the SCALE 6.1 code package.

		Temperature (Kelvin)									
		Spent Fuel Pool (Water @ 50 c = 324.15 k)					Cask (Helium @ 197.40 c = 471.55 k)				
		3 mos	6 mos	18 mos	36 mos	60 mos	3 mos	6 mos	18 mos	36 mos	60 mos
Fuel		2769.15	1314.15	738.15	525.15	441.15	3018.71	1503.38	902.61	681.07	593.83
He Gap		894.15	555.15	420.15	371.15	351.15	1143.87	743.91	585.34	526.86	503.84
Zirc4		430.02	367.15	342.15	333.15	329.15	679.73	555.89	506.79	488.69	481.56
Cd		374.13	344.15	332.15	328.15	326.15	623.83	533.25	497.33	484.09	478.88

Table 2: Temperatures used in simulations to determine keff.

Table 2 shows the temperatures used in the simulations. These temperatures were obtained from the outputs of the heat transfer calculations. The spent fuel pool water was assumed to be 50° Celsius, while the helium in the dry storage cask was assumed to be approximately 197° Celsius.

In Figure 12, K_{eff} calculated using SCALE is shown versus time at 3, 6, 18, 36, and 60 months in the spent fuel pool without the cadmium cladding shell on the fuel pins.

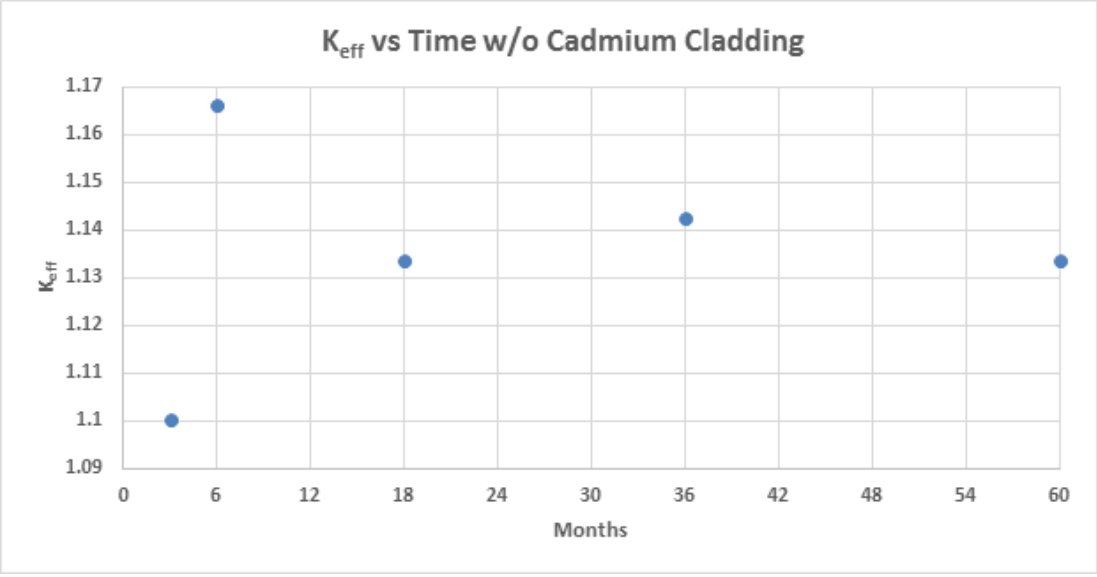

Figure 12: K_{eff} vs Time for the Fuel Assemblies in the cooling pool without the Cd Shell

Without the cadmium cladding shell on the fuel pins there does not appear to be a time dependence on K_{eff}. In Figure 13, K_{eff} calculated using SCALE is shown versus time at 3, 6, 18, 36, and 60 months in the spent fuel pool with the one mm thick cadmium cladding shell on the fuel pins.

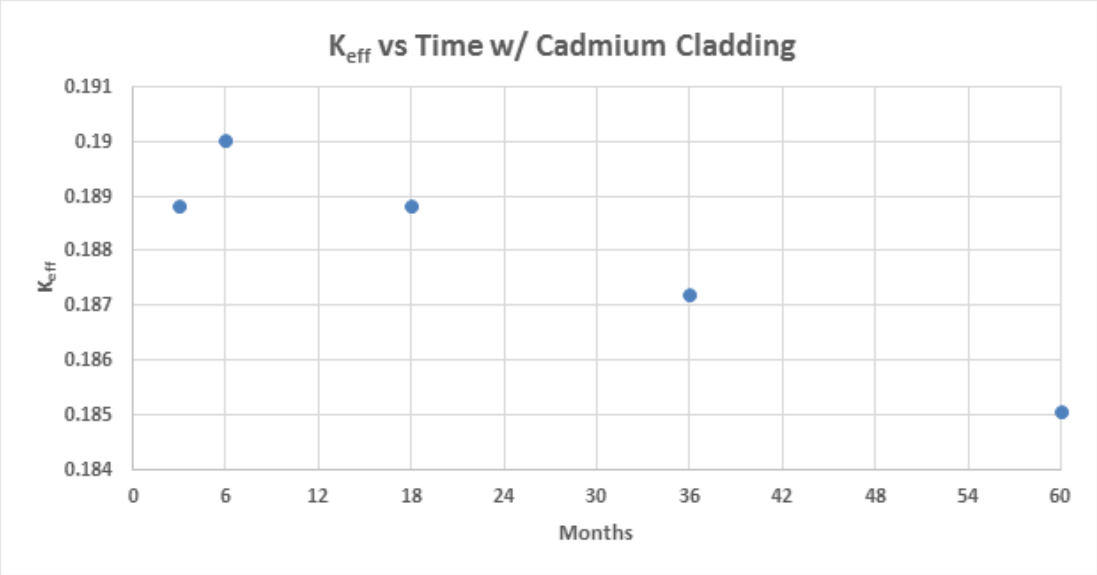

Figure 13: K_{eff} vs Time for the Fuel Assemblies in the cooling pool with the Cd Shell

With the cadmium cladding shell there seems to be a decrease in K_{eff} as time increases. There is a slight increase at the 6 month time interval, most likely caused by anomalies in the fission product compositions or resonances. In Figure 14, K_{eff} calculated using SCALE is shown versus variable thicknesses of the cadmium cladding shell on fuel pins in assemblies in the spent fuel pool.

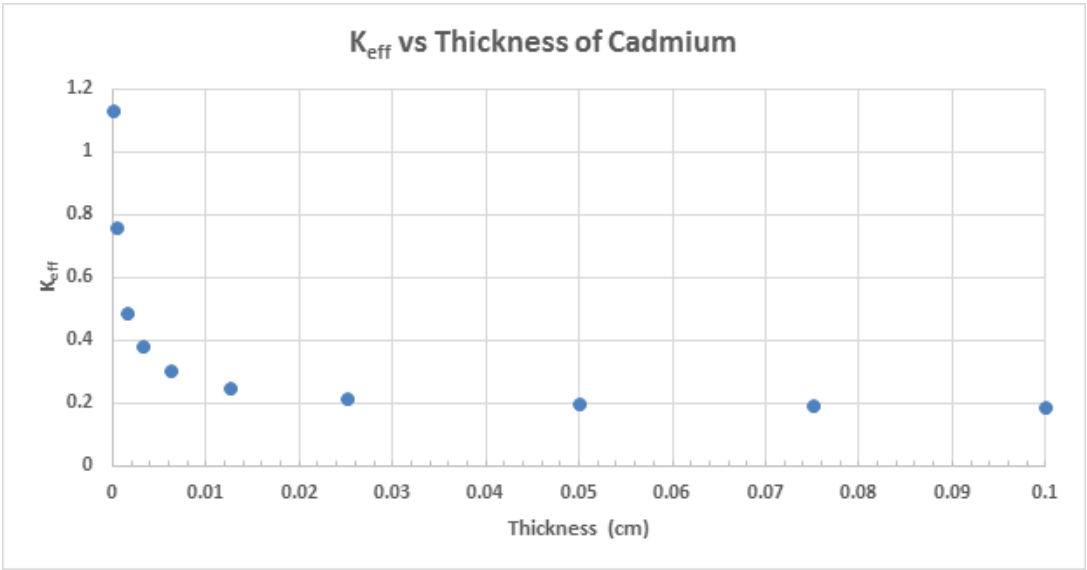

Figure 14: K_{eff} vs Thickness of the Cadmium Cladding Shell for the Fuel Assemblies in the Spent Fuel Pool

The results of these simulations show an exponential decrease in K_{eff} as the cadmium cladding shell thickness is increased. The K_{eff} reaches an asymptote at approximately 0.2 at a cadmium thickness of 0.025 cm.

In Figure 15, K_{eff} calculated using SCALE is shown versus time at 3, 6, 18, 36, and 60 months in the dry storage cask without the cadmium cladding shell on the fuel pins.

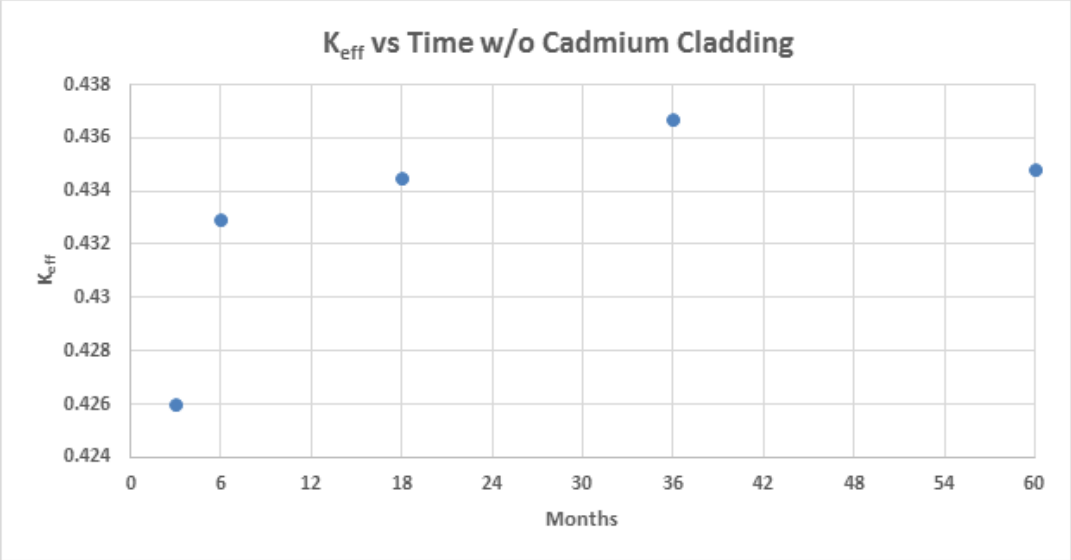

Figure 15: K_{eff} vs Time for the Fuel Assemblies in the NAC-I28 Dry Storage Cask without the Cadmium Cladding Shell

Without the cadmium cladding shell on the fuel pins there does not appear to be a time dependence on K_{eff}. In Figure 16, K_{eff} calculated using SCALE is shown versus time at 3, 6, 18, 36, and 60 months in the dry storage cask with the cadmium cladding shell on the fuel pins.

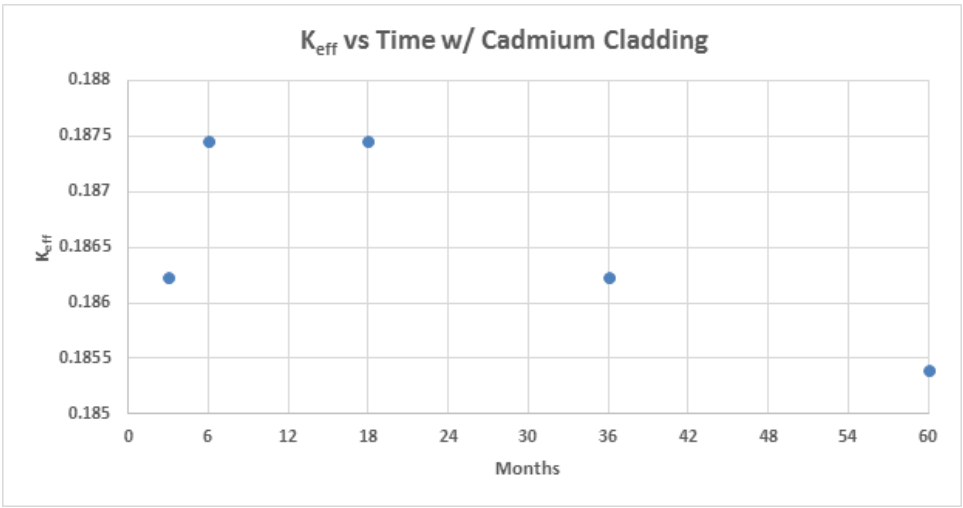

Figure 16: K_{eff} vs Time for the Fuel Assemblies in the NAC-I28 Dry Storage Cask with the Cadmium Cladding Shell

With the cadmium cladding shell there seems to be a decrease in K_{eff} as time increases. There is a slight increase and plateau at the 6 and 18 month time intervals, most likely caused by anomalies in the fission product compositions or resonances, as before. In Figure 17, K_{eff} calculated using SCALE is shown versus variable thicknesses of the cadmium cladding shell on fuel pins in assemblies in the dry storage cask.

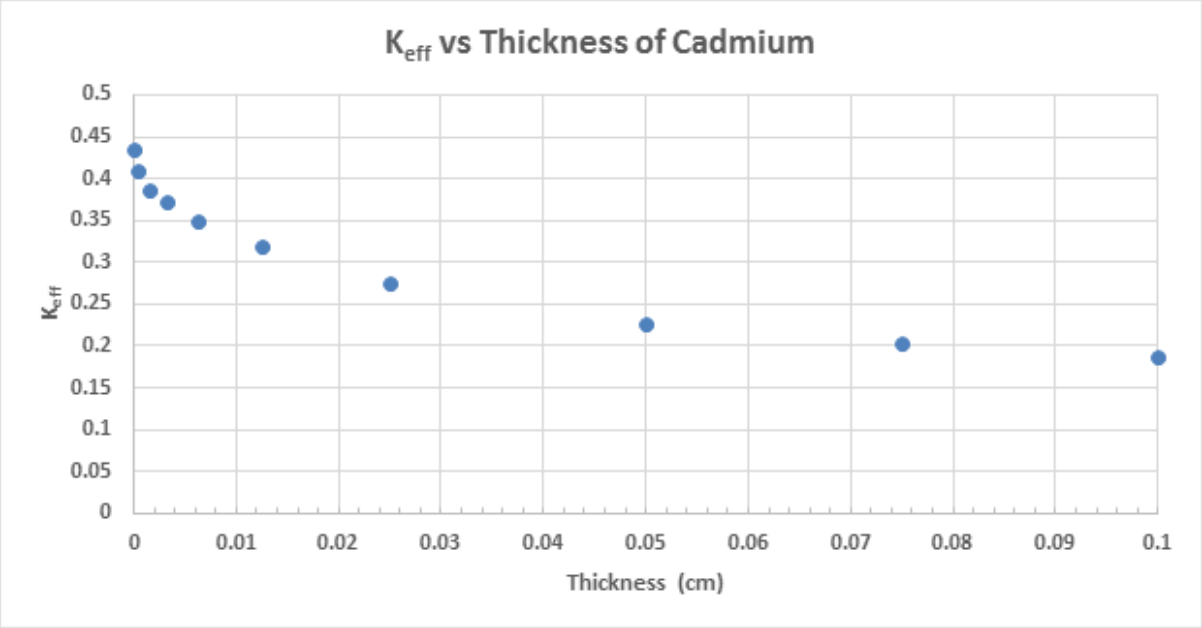

Figure 17: K_{eff} vs Thickness of the Cadmium Cladding Shell for the Fuel Assemblies in the NAC-I28 Dry Storage Cask

The results of these simulations show an exponential decrease in K_{eff} as the cadmium cladding shell thickness is increased. The K_{eff} reaches an asymptote at approximately 0.2 at a cadmium thickness of 0.05 cm. In Figure 18, the fission rate map for fuel assemblies within the spent fuel pool are shown as calculated using SCALE for fuel pins without a cadmium shell.

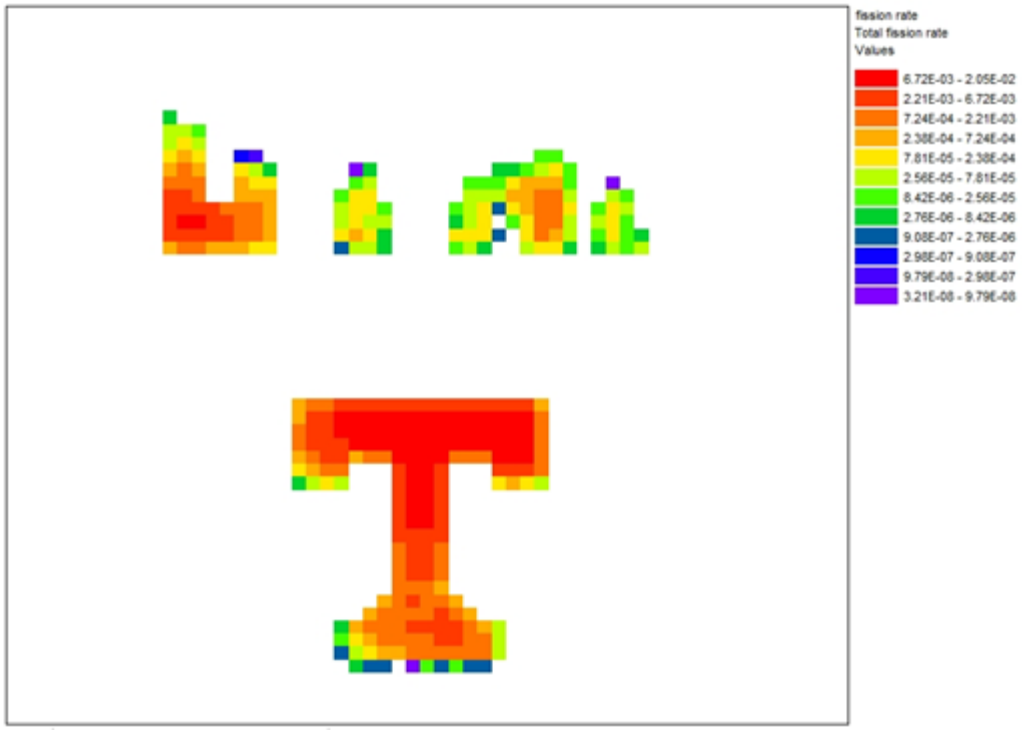

Figure 18: Fission Rate Map in Spent Fuel Pool with Fuel Assemblies without the Cadmium Cladding Shell

The results of the SCALE model show the varying total fission rates with the maximum being 2.05E-2 fissions per second and a minimum of 3.21E-8 fissions per second. Alternatively in Figure 19, a fission rate map for assemblies with a cadmium shell in the spent fuel pool is shown.

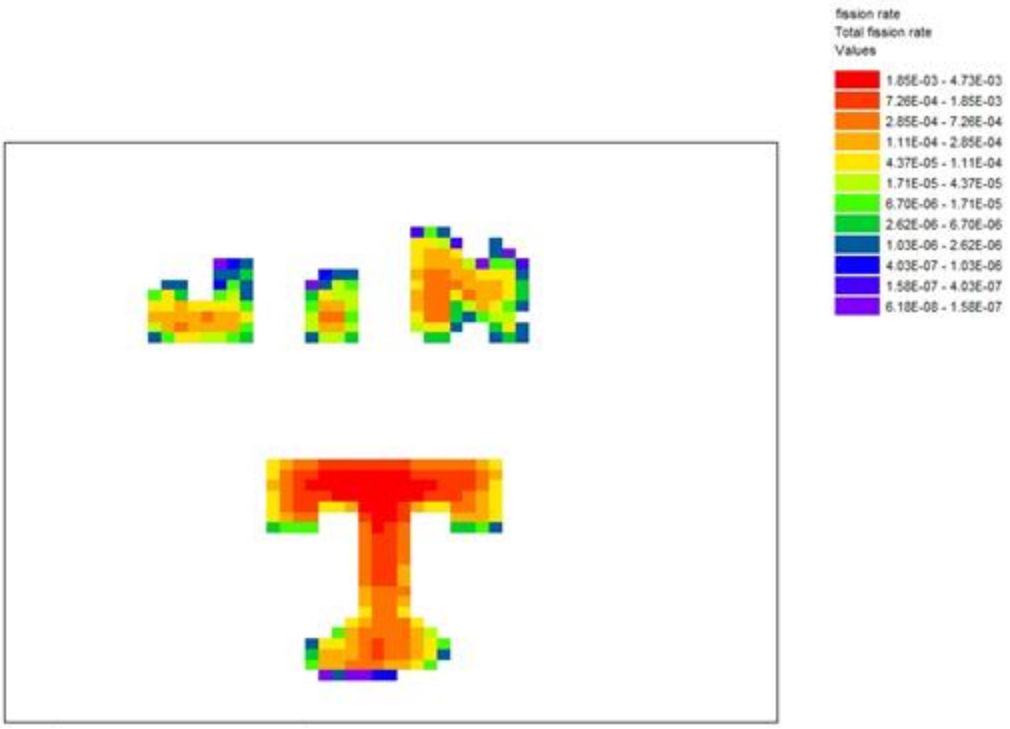

Figure 19: Fission Rate Map in Spent Fuel Pool with the Cadmium Cladding Shell

Reductions in fission rate can be seen as a result of the added cadmium cladding. The maximum in this case is 4.73E-3 fissions per second and the minimum is 6.18E-8 fissions per second. Visually, the addition of the cadmium makes the "E" disappear completely. In Figure 20, the fission rate map for fuel assemblies within the dry storage cask are shown as calculated using SCALE for fuel pins without a cadmium shell.

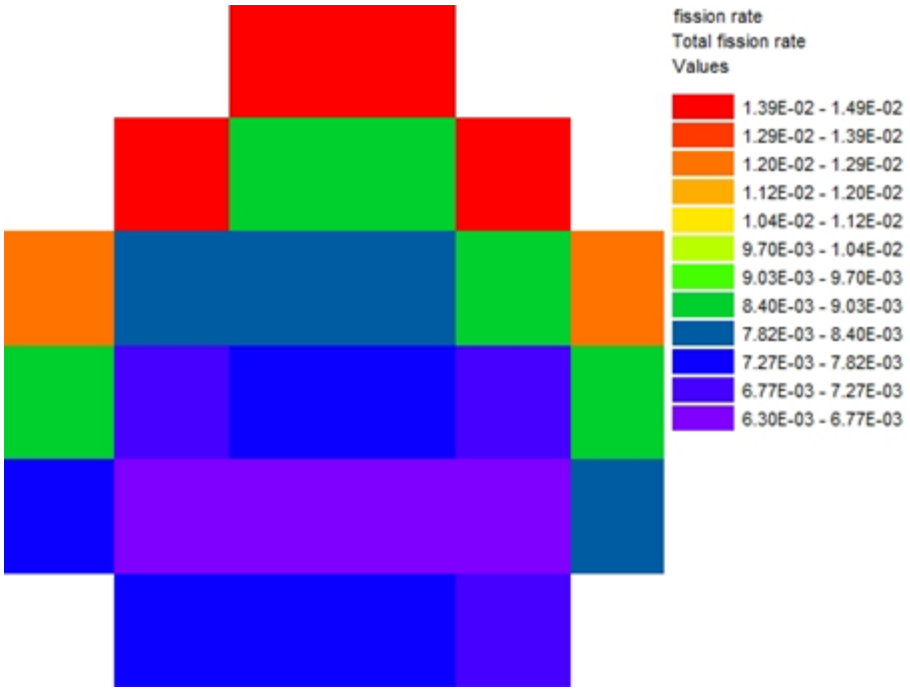

Figure 20: Fission Rate Map in Cask without the Cadmium Cladding Shell

The results of the SCALE model show the varying total fission rates with the maximum being 1.49E-2 fissions per second and a minimum of 6.30E-3 fissions per second. The hottest fuel assemblies in this case are on the outside edge with the most space between the fuel assemblies and the neutron absorber material of the cask. Alternately in Figure 21, a fission rate map for assemblies with a cadmium shell in the dry storage cask is shown.

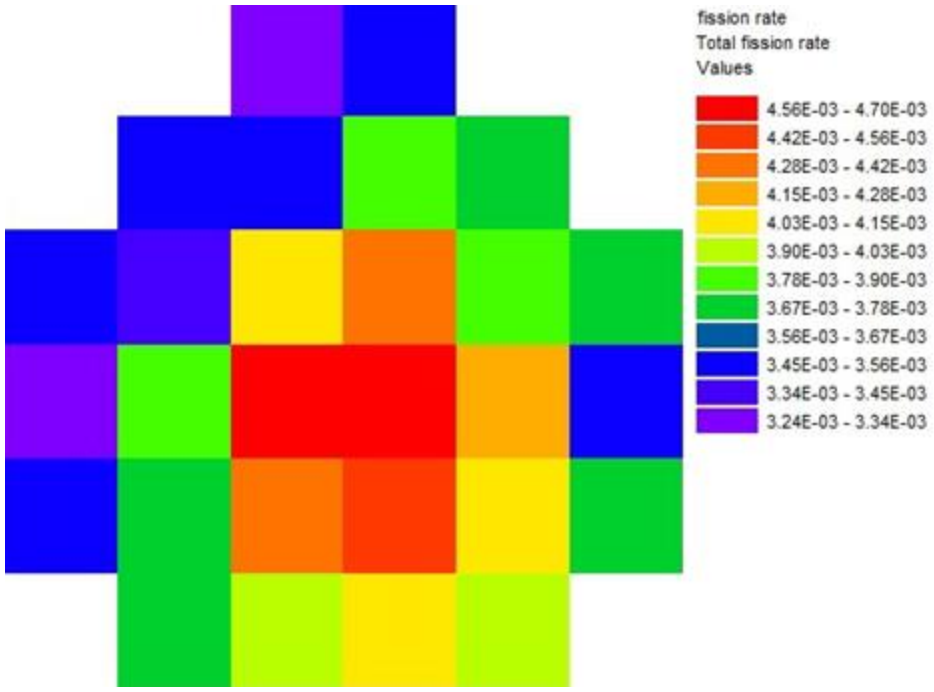

Figure 21: Fission Rate Map in Cask with the Cadmium Cladding Shell

Reductions in fission rate can be seen as a result of the added cadmium cladding. The maximum in this case is 4.70E-3 fissions per second and the minimum is 3.24E-3 fissions per second. The cadmium cladding on the assemblies appears to make the center assemblies the hottest.

6: Conclusion

Application of fuel assembly by means of dipping into a pure Cd metal succeeded in wetting the zircaloy rods. The thermal analysis shows that a Cd shell is safe to reside on an assembly in both the cooling pool and in dry cask storage. The calculations were performed using the maximum allowable temperature for each coolant, He and water. Therefore there is no concern that the shell would approach its melting point in any case but an accident scenario which is not considered in this work.

The criticality analysis examined the change in K_{eff} with the addition of a cadmium shell. With the addition of a 1 millimeter cadmium shell, the K_{eff} is reduced by approximately a factor of five in the spent fuel pool and by a factor of two in the dry storage cask. Therefore fuel coated in this shell achieves a reduction in reactivity that allows for spacing reduction in the cooling pool without the use of absorber plates in the racks. The results also show that Keff approaches a lower asymptote around cadmium shell thicknesses of 0.025 cm in the spent fuel pool and 0.05 in the dry storage cask. This implies that an uneven coating reducing the thickness to half of the total in spots would be a non-issue. From the fission rate maps, one can see that the cadmium does significantly decrease

the total fission rates in the assemblies; however it also seems to raise the average of the fission rate values. This could be because while the cadmium has a high thermal neutron cross section, the faster neutrons are being reflected back and causing the fission rates to stay higher.

Overall, the technique explored is proven feasible, and future development of the dipping process for used fuel assemblies is promising.

7: Future work

During the dipping process, the temporal temperature profile of the assembly is unknown. In other words, the amount of time available to keep the assembly in air before unsafe temperatures are reached is unknown. The heating changes with elapsed time after reactor removal as well. Perhaps the process is feasible soon after reactor removal, but this needs to be determined. A calculation using a software package such as COMSOL or a more sophisticated thermal analysis of the assembly in air is needed. The simplicity of the thermal analysis presented for other stages of the assembly's life here is recognized. A total reevaluation which is more rigorous would be performed as well.

A large scale experiment should be conducted to better understand the distribution of the shell once it is applied to an assembly. A first step could be to take a full-length zircaloy rod and dip it into Cd to observe the wetting along the length of the rod. If possible, a 17x17 array of zircaloy rods could be arranged to better emulate the behavior of an actual assembly. With that knowledge, criticality and thermal analyses may be performed to more accurately reflect the behavior of the Cd shell on a assembly which is still producing heat. Local accumulations of metal can compromise the assumptions made in the thermal analysis of the fuel rods. The thickness of the shell is on the same order of magnitude as the fuel rod pitch. Therefore there are concerns that the cadmium could pool and accumulate between rods, forming a mechanical connection between rods that has not been considered. Additionally, more alloys would be tested for their ability to wet on zircaloy. While it is unlikely that a better neutron absorber than cadmium would be found to be suitable, but perhaps an alloy with a lower cross section wets and deposits along the surface of the fuel cladding better than cadmium.

References

1: NRC, www.nrc.gov

2: Ceradyne Inc., http://www.ceradyneboron.com/products/nuclear-power/neutron-absorbers/boral/

3: "Welcome to SCALE." *SCALE*. ORNL. Web. 24 Apr. 2014. <http://scale.ornl.gov/>.

4: Pramuditya, Syeilendra. "Standard PWR Nuclear Fuel Assembly (17x17) Technical Specification." Web log post. *Hey Whats Going on*. 14a Apr. 2009. Web. 24 Apr. 2014.

5: *Scale: A Comprehensive Modeling and Simulation Suite for Nuclear Safety Analysis and Design*,ORNL/TM-2005/39, Version 6.1, June 2011. Available from Radiation Safety Information Computational Center at Oak Ridge National Laboratory as CCC-785.

6: Batalo, D. P., and B. H. Wakeman. *Design and Operation of the NAC-I28 Spent-Fuel Storage Cask*. Rep. no. TR-101091. Palo Alto: EPRI, 1992. Print.

7: Grossbeck, M. *Soldering and Brazing*. 2014. Powerpoint

Appendix I - Specific Inputs for FORTRAN Program

50	5	5	5	increments in fuel, gap, clad, and shell
0.528	0.008	0.0864	0.08	fuel radius, gap, clad, and shell thickness
0.025	0.004	0.107	0.2	thermal conductivities
10.0	0.4	6.56	7.00	densities (gas factor of 100 high)
0.32	10.0	0.28	0.3	specific heats
500.0				steady-state linear heat rate
290.0				steady-state coolant temperatures
5.000				steady-state coefficients
0				option: 0 = fixed k-fuel, 1 = variable k-fuel
0.01				temperature convergence criterion
1000				max number iterations to converge